JOURNAL OF CRITICAL REVIEWS

ISSN- 2394-5125 VOL 7, ISSUE 19, 2020

CFD INVESTIGATIONS ON THE CIRCULAR, RECTANGULAR AND ELLIPTICAL SHAPES ON AERODYNAMICS IN AN S-DUCT

1.Aravind s 2. M. Ramesh Kumar 3. Karthick b

1,3 – Assistant Professor , Department of Aeronautical Engineering

2 - Assistant Professor , Department of Mechanical Engineering

Dhanalakshmi Srinivasan College Of Engineering & Technology - Mamallapuram

[2]*rameshkumarm.mech@dscet.ac.in*

*1*aravindaero91@gmail.com

*3*karthickb@gmail.com

ABSTRACT;

A fully parametric 3D model (Solidworks) of the intake was constructed in order to produce different intake configurations, within specific geometric constraints, and to study the influence of Geometry cross sectional variation on efficiency. Cylindrical type, Rectangle- type and Ellipse- type blocking methodology was adopted in order to construct the block structured mesh of hexahedral elements, used in the simulations. The commercial CFD code ANSYS CFX was used to compute the flow field inside the flow domain of each case considered. The CFD analysis determines the Pressure, velocity, Kinetic energy, Density, Drag and lift forces. By shortening the axial length the flow separation after the first turning becomes more pronounced and the losses are increasing. For very long ducts the increased internal wall area leads to increased wall friction and consequently, to increased loss production.

INTRODUCTION

Engine performance and stability margin are affected also by inlet flow losses and distortion, which mainly depend on the inlet geometry, aircraft flight condition and engine airflow. Therefore, an estimation of inlet performance is important for an improved simulation of engine performance.

For a fuselage-embedded engine, a curved diffuser called an S-duct or S-bend is used to route air from the side of the flight vehicle to the interior and is therefore an important part of the inlet. The design of the inlet and consequently the design of the S-duct diffuser vary from one flight vehicle to another depending upon the engine location, airframe configuration, and flight environment. The performance of various types of S-duct diffusers is available in the open literature.The latter two are defined at a common instrumentation plane between the inlet duct and the engine and is termed the Aerodynamic Interface Plane (AIP).

The AIP is located a short distance upstream of the engine face. The location of the AIP is generally agreed upon by the engine and airframe manufacturers and all the measurements (in wind tunnels or by CFD models and in flight tests on prototypes) are carried out at this plane.

ISSN- 2394-5125 VOL 7, ISSUE 19, 2020

The flow in the S-duct diffuser is complex due to two or more curves in the duct and to changes, sometime abrupt, in the cross-section area and shape.

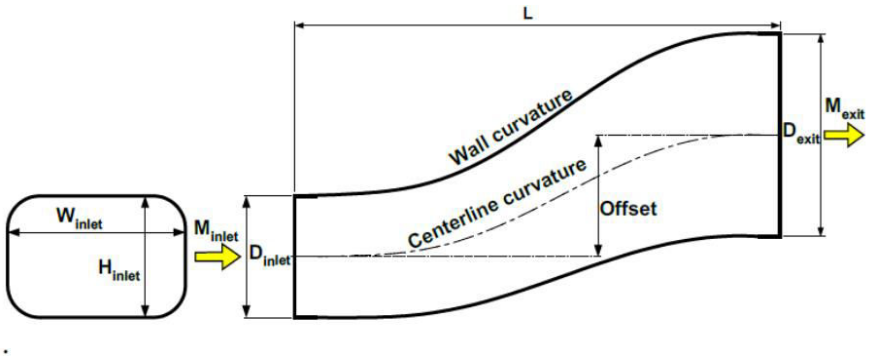

Fig: 1.1 S-duct diffuser

The important geometric characteristics of an S-duct diffuser, as shown in Fig. 1.1, are the center-line curvature, the wall curvature profile, the area ratio between the exit and entrance cross section, axial length and offset.

The cross sectional shape of an inlet can transition from rectangular, oval, etc. at the entrance to circular at the engine face. The duct centre line curvature can have different turning angles and shapes. The design varies depending upon the complete flight vehicle configuration. However, in general, two types of S-ducts are more common in the open literature. In the early 1980s, the RAE M2129 was introduced by researchers at British Aerospace Industries. The M2129 S-duct is described by the centreline curvature and wall profile equation using Cartesian coordinates. The usual offset and length ratio based on the exit, or engine face, diameter are 0.9 and 3, respectively. Similarly, in the early 1980s, a two equal-arc design, e.g. NASA 30/30 was introduced by researchers at NASA and the University of Tennessee Space Institute and is characterized by the centerline curvature and wall profile equation (for circular cross-sections) with the radius and angle of curvature as independent parameters. The approximate offset and length ratio based on the exit diameter are 0.8-0.9 and 3-4, respectively.

Colin Fiola and Ramesh K Agarwal[1] on the numerical simulation of compressible flow in a diffusing S-duct inlet; this flow is characterized by secondary flow as well as regions of boundary layer separation. The S-duct geometry produces streamline curvature and an adverse pressure gradient resulting in these flow characteristics. The geometry used in this investigation is based on a NASA Glenn Research Center experimental diffusing S-duct. The computational fluid dynamics flow solver ANSYS - FLUENT is employed in the investigation of compressible flow through the S-duct. A second-order accurate, steady, density-based solver is employed in a finite-volume framework. The three-dimensional Reynolds-Averaged Navier-Stokes equations are solved on a structured mesh with a number of turbulence models, namely the Spalart–Allmaras (SA), k-", k-! SST, and Transition SST models, and the results are compared with the experimental data.

K. M. Britchford, A. P. Manners, J. J. McGuirk, S. J. Stevens et al[2] Annular S-shaped ducts are often used as interconnecting ducts between compressor spools in modern gas turbine engines. Duct curvature and the presence at inlet of wakes emanating from upstream

ISSN- 2394-5125 VOL 7, ISSUE 19, 2020

compressor blading exert a strong influence on flow development. Measurements indicate that with a compressor stage at inlet the tendency for the flow along the inner wall to separate is reduced. This effect is attributed in part to a reenergizing of the inner wall boundary layer brought about by the inward radial pressure force driving the blade wake flow into the wall region. CFD predictions of the clean inlet case using k-e and Reynolds stress transport turbulence models demonstrate that only the second moment closure captures the curvature effects adequately. Even then discrepancies are still observed.

CaglarAtalayer, Jens Friedrichs and DetlevWulff[3] in this the conceptual integration process, sensitivity analysis based on the intake performance has been done to identify the limitations on the S-duct geometry using computational methods. The flow simulations were done on an isolated, uninstalled S-duct intake, excluding propeller effects and particle separator, for an initial specification in advance of the actual sizing. The effects of fundamental geometric features, as the intake aspect ratio, duct lengths and spread angle, were investigated on the flow quality through the aerodynamic interface plane (AIP), quantified by total pressure recovery and distortion.

Asad Asghar, Robert A. Stowe, William D.E. Allan and Derrick Alexander[4] in this the generic baseline was a rectangular-entrance, transitioning S-duct diffuser in high subsonic (Mach number > 0.8) flow. The test section was manufactured using rapid prototyping for facilitating a future parametric investigation of geometry. Stream wise static pressure and exit-plane total pressure were measured in a testing using surface pressure taps and a 5-probe rotating rake, respectively and was simulated through computational fluid dynamics. The investigation indicated the presence of stream wise and circumferential pressure gradients leading to three dimensional flow in the S-duct diffuser and distortion at the exit plane. Total pressure losses and circumferential and radial distortions at the exit plane were higher than that of the podded nacelle type of inlet.

Mats Dalenbring and Jonathan Smith[5] in this the design of S-duct channels is complicated since the internal curvature can result in regions of unsteady, separated flow which endanger engine performance. Such effects may be countered by static flow-control using vortex generator (VG) arrays. For this, specialised CFD-based design techniques 4 have been developed. However, almost all CFD-studies to date have been restricted to steady-state flow solutions for rigid surface geometries. Due to the sensitivity of the internal flow to the channel geometry and the need for extreme lightweight construction,

It is also necessary to account for dynamic aero elastic effects. This article presented a series of three-dimensional aero elastic simulations using structure-coupled CFD and demonstrated that it is possible to use these methods to re-design an S-duct system, improving both structural efficiency and the stability of the internal flow.

The structural design of the Eikon S-duct channels is constrained by the need to balance low-observability requirements on visual, Infra-Red and radar signatures. For this, the shielding effect of the S-duct is enhanced by using specialised Infra-Red and radar absorbing materials (RAM) and radar absorbing structures (RAS). This has been described elsewhere in the wider context of stealth aircraft technology.

ISSN- 2394-5125 VOL 7, ISSUE 19, 2020

Anne-Laure Delot[6] in this results were generated for the first AIAA Propulsion Aerodynamics Workshop (PAW01) using different codes, grids, turbulence models, and computers. Examples of computational grids for unstructured and structured solvers were provided by the PAW01 committee to each participant. The geometry of the test case was also provided for those interested in developing their own grids. This paper summarizes the results from that first workshop and documents the effects of grid refinement, symmetry boundary conditions, turbulence models, and codes used by the various participants from across industry and academia. The CFD studies were performed as a blind trial and are compared with the available experimental data during the workshop.

WenbiaoGana,,Xiaocui Zhang[7] in this the design optimization of a three-dimensional diffusing S-duct using a modified k shear stress transport (SST) turbulent model as a turbulence prediction method. According to Reynolds-stress and based-separation ideas, a robust solution procedure for the model is described and a grid convergence study is presented. An automated system employs this model to design a S-duct. The aerodynamic performances of the optimal duct are investigated in on-design and off-design conditions.

It is shown that the sensitivity of the modified model with respect to shape variations allows its use in the design system. Using a multi-objective optimization strategy, this design system significantly improves aerodynamic performance of the S-duct and has low computation cost and excellent design efficiency. The centreline's curvature and the cross-sectional area ratio become reasonable to avoid over expand of the optimal duct. Compared with the original design, the flow distortion coefficient of the optimal duct is reduced by 16.3% and the total pressure recovery factor is increased by 1.1% in on-design condition.

Andrea Garbo and Brian J. Germany[8] on the design process that enables a qualitative and quantitative understanding of physical phenomena, trades, and constraints. Additionally, design space exploration can be used to create surrogate models for later design and optimization tasks. For large design spaces that are explored with computationally expensive tools such as CFD or FEM, the design space exploration method must be efficient to obtain a good representation of the trade space with relatively few sampled design points. Several design space exploration methodologies and approaches are described in the literature, including a priori sampling approaches, adaptive methods, and multi fidelity strategies. The main goal of the present paper is to conduct a comparison of some of these methodologies to understand their exploration behavior and efficiency when used with high _fidelity and computationally expensive simulation tools. This goal is achieved by applying the methods to the same test case: a design space exploration of the internal aerodynamics of s-duct geometries to assess pressure loss performance. The aerodynamic analysis is conducted with a viscous 3-D CFD solver that allows multi- fidelity results to be easily obtained by changing the mesh density.

Manoj Kumar Gopaliya, Mahesh Kumar[9] in this the effect of offset (i.e. inlet and outlet are in two different planes) on S-shaped diffuser of 90◦/90◦turn with rectangular inlet (AS = 2) and semicircular outlet (AR=2). A computer program based on finite volume technique,

ISSN- 2394-5125 VOL 7, ISSUE 19, 2020

using standard k–ε turbulence 18 model, has been adopted and modified to predict the flow. The obtained results from this research show reduced outlet pressure recovery accompanied with increase in non-uniformity at the exit due to offset. This paper also shows that increase in Reynolds number has marginal effect on the outlet pressure recovery for zero offset and 0.3125D cases and similar results have been found for other offset cases which have not been presented in the paper to avoid repeatability. The present S-duct geometry fulfills only pressure recovery requirement, and hence needed modification to improve the uniformity at the exit.S. Lavagnoli, T. Yasa, G. Paniagua, S. Duni [10] in this the aerodynamics of an innovative multisplitter LP stator downstream of a high-pressure turbine stage is presented. The stator row, located inside a swan necked diffuser, is composed of 16 large structural vanes and 48 small airfoils. The experimental characterization of the steady and unsteady flow field was carried out in a compression tube rig under engine representative conditions. The one-and-a-half turbine stage was tested at three operating regimes by varying the pressure ratio and the rotational speed. Time-averaged and time-accurate surface pressure measurements are used to investigate the aerodynamic performance of the stator and the complex interaction mechanisms with the HP turbine stage. Results show that the strut blade has a strong impact on the steady and unsteady flow field of the small vanes depending on the vane circumferential position Methodology

The main flow domain of the S-duct (from duct inlet to the engine face) was modelled in CATIA V5, as described earlier, and imported to ANSYS ICEM CFD commercial mesh generation software. An additional cylindrical part, common to all cases considered, containing engine inlet and the corresponding engine bullet, was constructed.

➢ Its axial length Lax,eng was set equal to 300 mm. The bullet was constructed as a rounded cone with a base diameter Dbul equal to 50 mm Def and a height Lax,bul equal to 1.288Dbul.

➢ The rounded of the bullet was constructed using a spherical sector, in a way to maintain curvature continuity between the sphere and the cone at their interface.

➢ Rectangle section axial length Lax,eng was set equal to 300 mm. The rectangle with a base diameter length L is 65.4 mm breadth B 30 mm and a height Lax,bul equal to 1.288B.

➢ Ellipse section axial length Lax,eng was set equal to 300 mm. The ellipse with a base diameter length A is 20.8 mm breadth B 30 mm and a height Lax,bul equal to 1.288A.

➢ Cylindrical section, Rectangular section and Ellipse section blocking methodology was used in order to construct the mesh, used in our simulations; the mesh consists of hexahedral elements.

➢ The adopted blocking strategy consists of making blocks for the primitive and general geometrical features and continuing to the most detailed and smaller parts of the geometry.

ISSN- 2394-5125 VOL 7, ISSUE 19, 2020

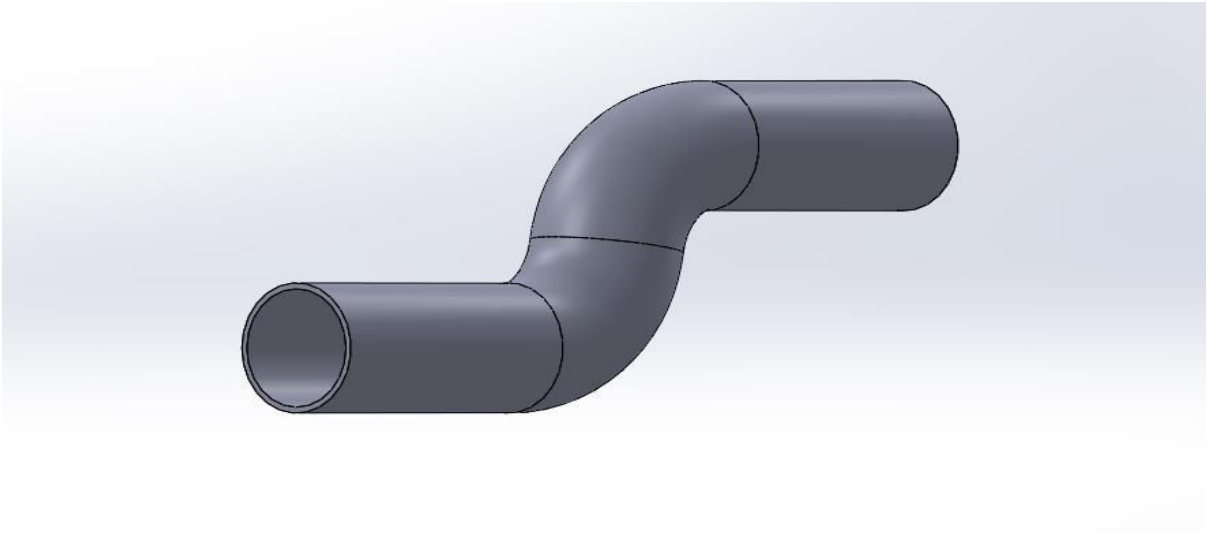

Fig:4.1 CAD Model of Circular S- Duct Design

.

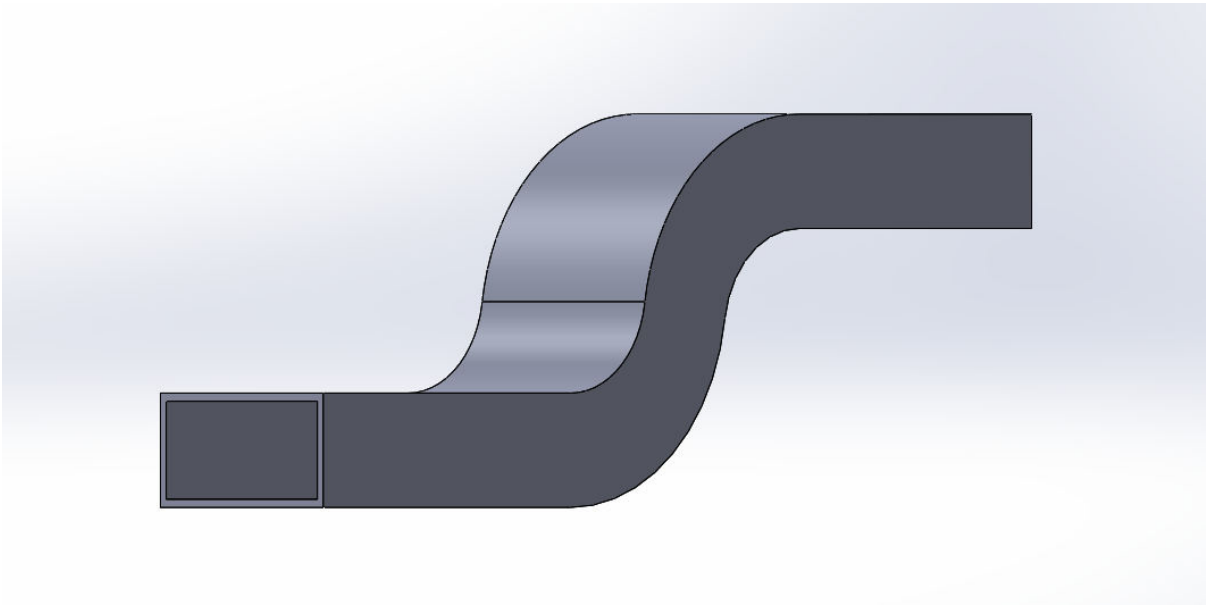

Fig:4.2 CAD Model of Rectangular S- Duct Design

ISSN- 2394-5125 VOL 7, ISSUE 19, 2020

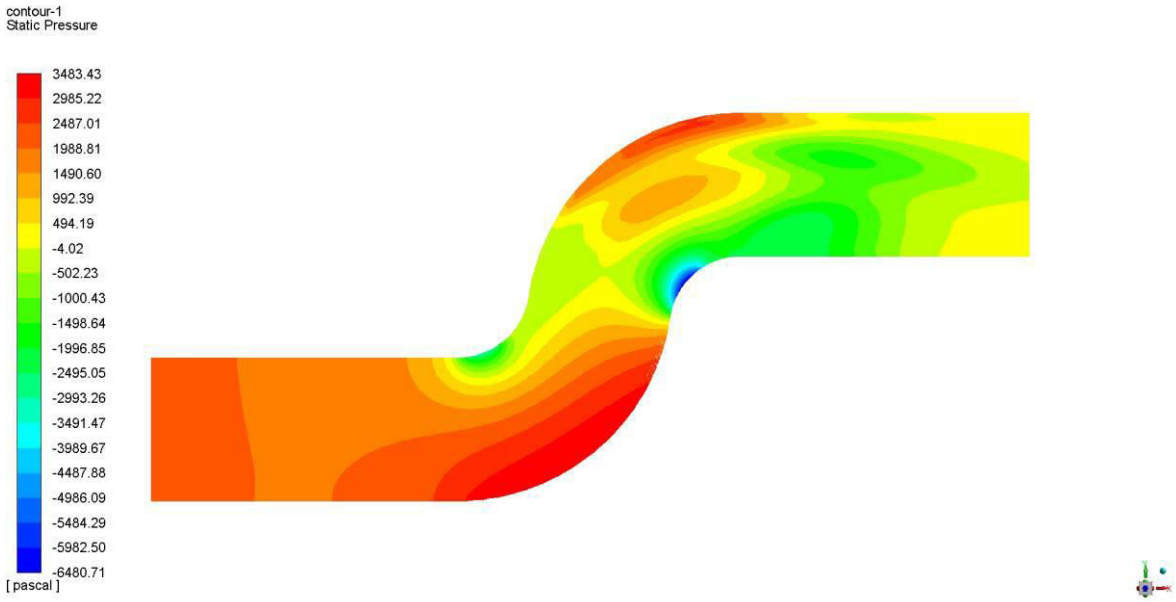

Fig:4.5 CFD analysis of Circular S-Duct Static Pressure

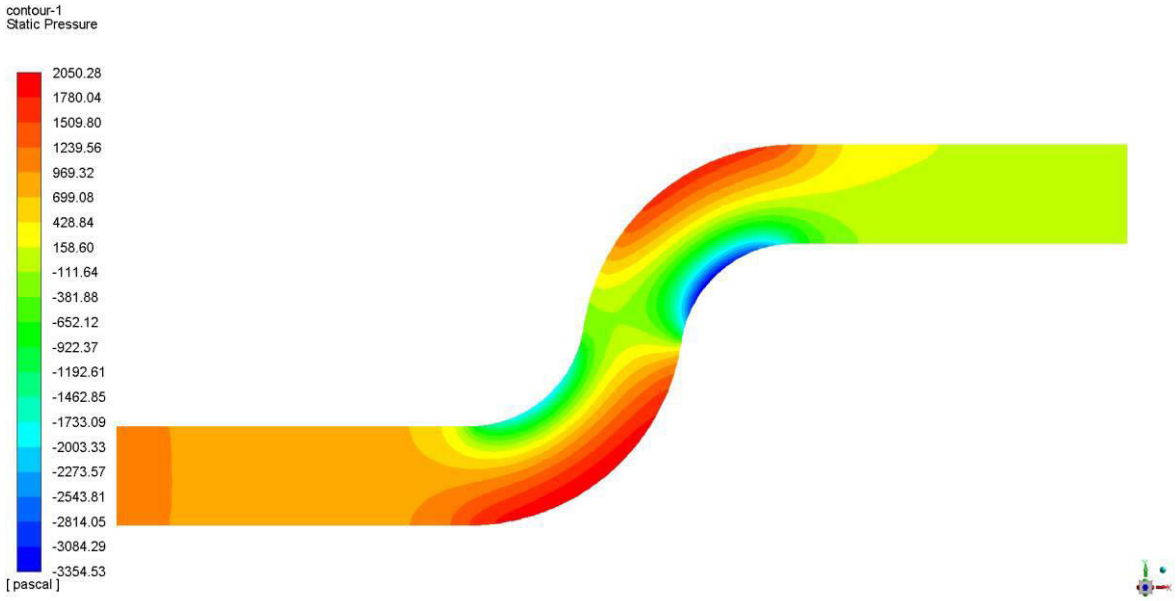

Fig:4.6 CFD analysis of Rectangular S-Duct Static Pressure

ISSN- 2394-5125 VOL 7, ISSUE 19, 2020

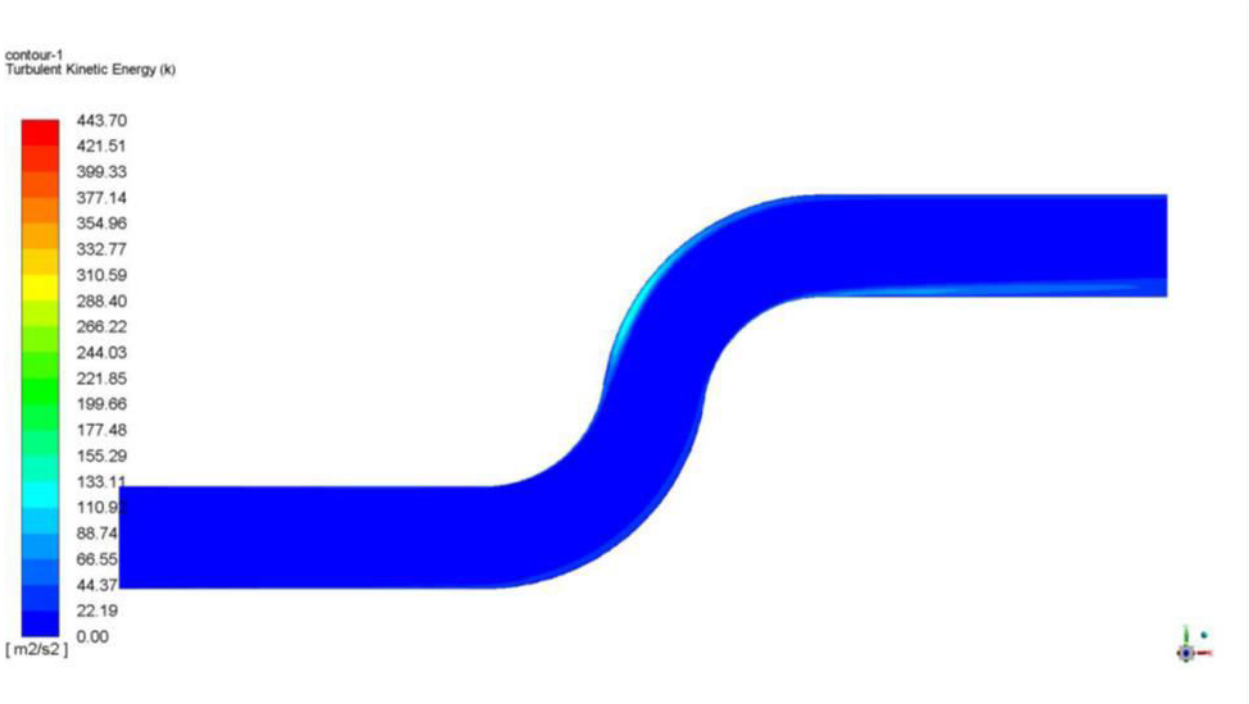

Fig:4.9 CFD analysis of Rectangular S-Duct Turbulent Kinetic Energy (k)

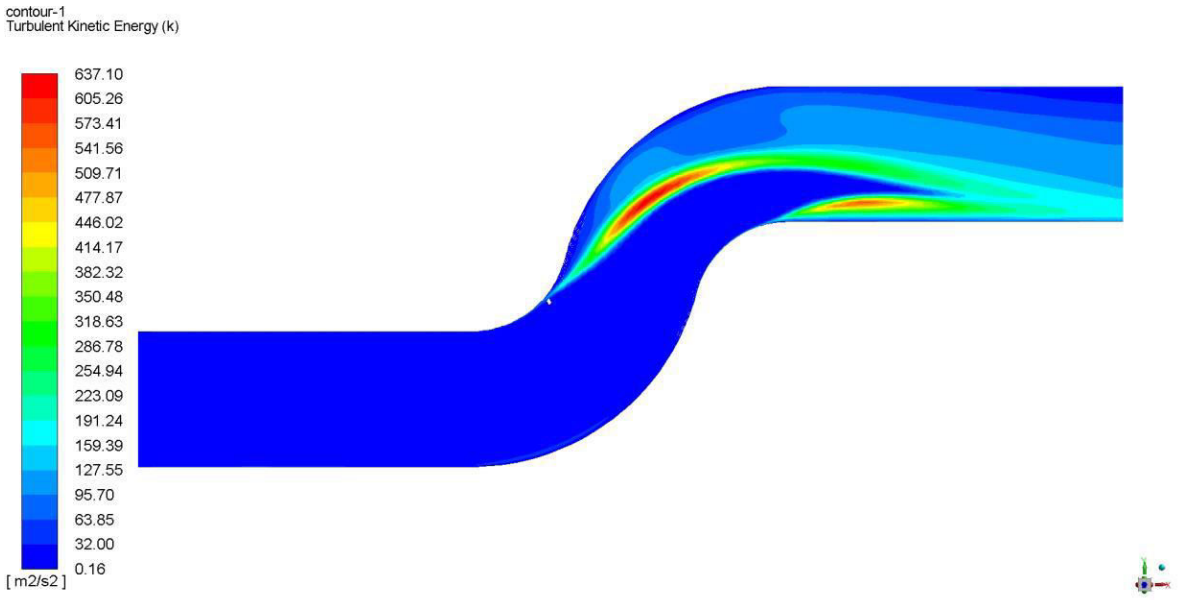

Fig:4.10 CFD analysis of Ellipse S-Duct Turbulent Kinetic Energy (k)

Fig:4.17 CFD analysis of Circular S-Duct Drag force

Forces - Direction Vector (1 0 0)

	Forces (n)			Coefficients		
Zone	Pressure	Viscous	Total	Pressure	Viscous	Total
wall	2.8380505	0.72164377	3.5596943	0.00096093631	0.00024434156	0.0012052779
Net	2.8380505	0.72164377	3.5596943	0.00096093631	0.00024434156	0.0012052779

ISSN- 2394-5125 VOL 7, ISSUE 19, 2020

Fig:4.18 CFD analysis of Circular S-Duct Lift force

Forces - Direction Vector (0 1 0)

	Forces (n)			Coefficients		
Zone	Pressure	Viscous	Total	Pressure	Viscous	Total
wall	-0.049984038	0.27187953	0.22189549	-1.6924109e-05	9.2055766e-05	7.5131656e-05
Net	-0.049984038	0.27187953	0.22189549	-1.6924109e-05	9.2055766e-05	7.5131656e-05

Fig:4.19 CFD analysis of Rectangular S-Duct Drag force

Forces - Direction Vector (1 0 0)

	Forces (n)			Coefficients		
Zone	Pressure	Viscous	Total	Pressure	Viscous	Total
wall	0.9976384	0.78216883	1.7798072	0.00033779066	0.00026483476	0.00060262542
Net	0.9976384	0.78216883	1.7798072	0.00033779066	0.00026483476	0.00060262542

Fig:4.20 CFD analysis of Rectangular S-Duct Lift force

Forces - Direction Vector (0 1 0)

	Forces (n)			Coefficients		
Zone	Pressure	Viscous	Total	Pressure	Viscous	Total
wall	-0.2412335	0.22318187	-0.018051628	-8.1679318e-05	7.5567212e-05	-6.1121058e-06
Net	-0.2412335	0.22318187	-0.018051628	-8.1679318e-05	7.5567212e-05	-6.1121058e-06

Fig:4.21 CFD analysis of Ellipse S-Duct Drag force

Forces - Direction Vector (1 0 0)

	Forces (n)			Coefficients		
Zone	Pressure	Viscous	Total	Pressure	Viscous	Total
wall	1.5456017	0.70595325	2.251555	0.00052332572	0.00023902891	0.00076235463
Net	1.5456017	0.70595325	2.251555	0.00052332572	0.00023902891	0.00076235463

Fig:4.22 CFD analysis of Ellipse S-Duct Lift force

Forces - Direction Vector (0 1 0)

	Forces (n)			Coefficients		
Zone	Pressure	Viscous	Total	Pressure	Viscous	Total
wall	-0.30695751	0.21489177	-0.092065736	-0.00010393283	7.2760265e-05	-3.1172563e-05
Net	-0.30695751	0.21489177	-0.092065736	-0.00010393283	7.2760265e-05	-3.1172563e-05

Forces - Direction Vector (1 0 0)						
	Forces Pressure (n)	Viscous	Total	Coefficients Pressure	Viscous	Total
Zone Wall	2.955654700	0.752144500	3.707799200	0.000998755	0.000312478	0.001311233
Net	2.955654700	0.752144500	3.707799200	0.000998755	0.000312478	0.001311233

Forces - Direction Vector (1 0 0)						
	Forces Pressure (n)	Viscous	Total	Coefficients Pressure	Viscous	Total
Zone Wall	4.25896486	0.99878965	5.25775451	0.000478966	0.000457896	0.000936862
Net	4.25896486	0.99878965	5.25775451	0.000478966	0.000457896	0.000936862

Fig:CFD analysis of Ellipse S-Duct Drag force(350km)

ISSN- 2394-5125 VOL 7, ISSUE 19, 2020

Forces - Direction Vector (0 1 0)						
	Forces Pressure (n)	Viscous	Total	Coefficients Pressure	Viscous	Total
Zone Wall	-0.0678965	0.35777896	0.28988246	-2.3479E-05	8.78965E-05	6.44175E-05
Net	-0.0678965	0.35777896	0.28988246	-2.3479E-05	8.78965E-05	6.44175E-05

Fig:CFD analysis of an Ellipse S-Duct drag force(350km)

Forces - Direction Vector (1 0 0)						
	Forces Pressure (n)	Viscous	Total	Coefficients Pressure	Viscous	Total
Zone Wall	9.2563478	1.78965455	11.04600235	0.000897652	0.000456896	0.001354548
Net	9.2563478	1.78965455	11.04600235	0.000897652	0.000456896	0.001354548

FIG:CFD analysis of an Ellipse S-Duct Drag force(450km)

Forces - Direction Vector (0 1 0)						
	Forces Pressure (n)	Viscous	Total	Coefficients Pressure	Viscous	Total
Zone Wall	-0.5478962	0.357896577	-0.18999962	-1.2459E-06	9.12457E-06	-1.03705E-05
Net	-0.5478962	0.357896577	-0.18999962	-1.2459E-06	9.12457E-06	-1.03705E-05

FIG:CFD analysis of an ellipse S-Duct Drag force(450km)

ANALYSIS OF STATIC PRESSURE AT 200Km/HR

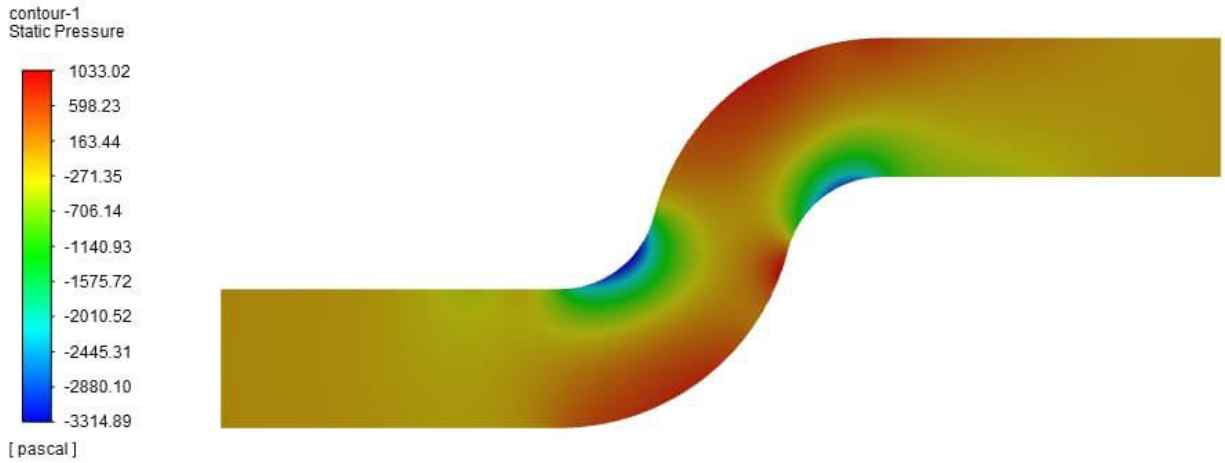

ANALYSIS OF FORCES IN X DIRECTION

```
Forces - Direction Vector (1 0 0)
                          Forces (n)                                    Coefficients
Zone                      Pressure        Viscous         Total         Pressure        Viscous         Total
wall                      1.4411972       0.64063196      2.0818291     0.00076236266   0.00033888069   0.0011012434
------------------------- --------------- --------------- ------------- --------------- --------------- ---------------
Net                       1.4411972       0.64063196      2.0818291     0.00076236266   0.00033888069   0.0011012434
```

ISSN- 2394-5125 VOL 7, ISSUE 19, 2020

ANALYSIS OF FORCE IN Y-DIRECTION

Forces - Direction Vector (1 0 0)

	Forces (n)			Coefficients		
Zone	Pressure	Viscous	Total	Pressure	Viscous	Total
wall	1.4411972	0.64063196	2.0818291	0.00076236266	0.00033888069	0.0011012434
Net	1.4411972	0.64063196	2.0818291	0.00076236266	0.00033888069	0.0011012434

ANALYSIS OF VELOCITY MAGNITUDE AT 200Km/HR

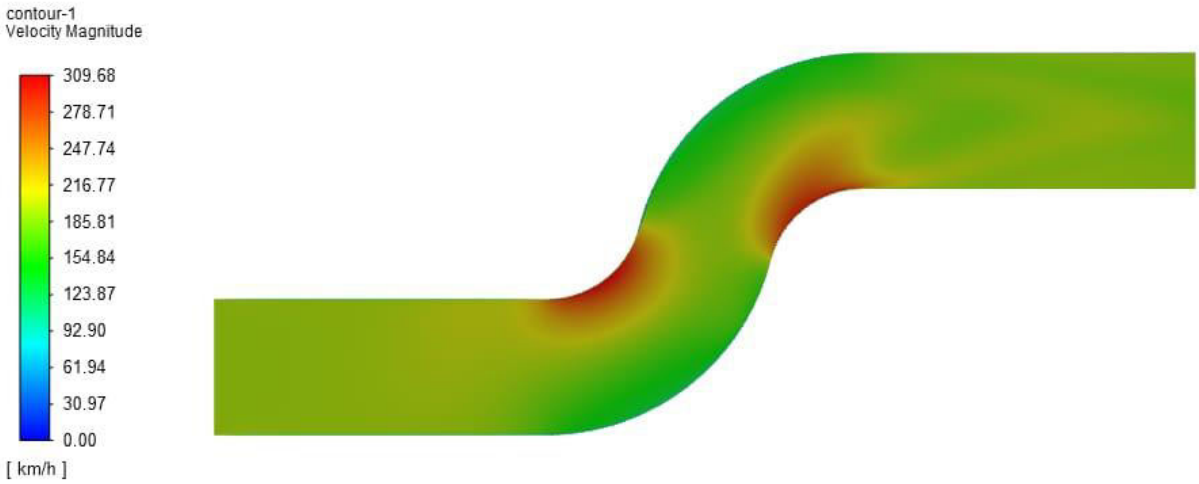

ANALYSIS OF TUBULENT KINETIC ENERGY AT 200Km/HR

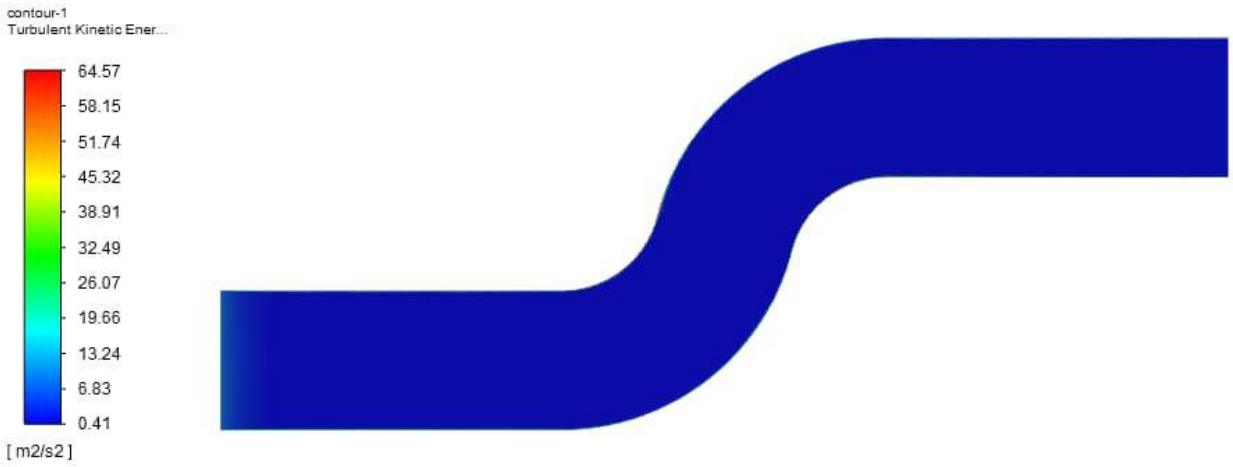

ISSN- 2394-5125 VOL 7, ISSUE 19, 2020

ANALYSIS OF VELOCITY MAGNITUDE AT 2OOKm/HR

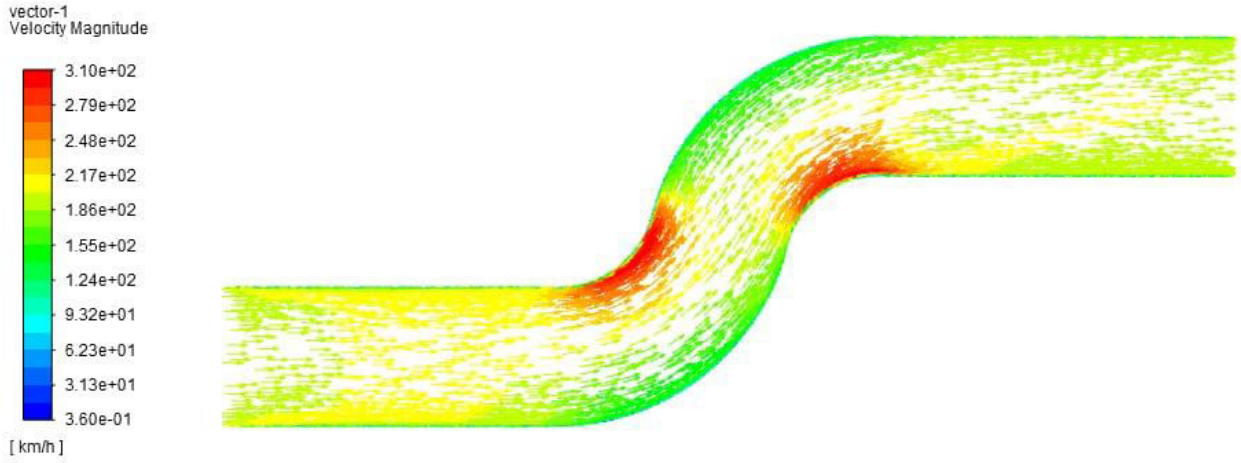

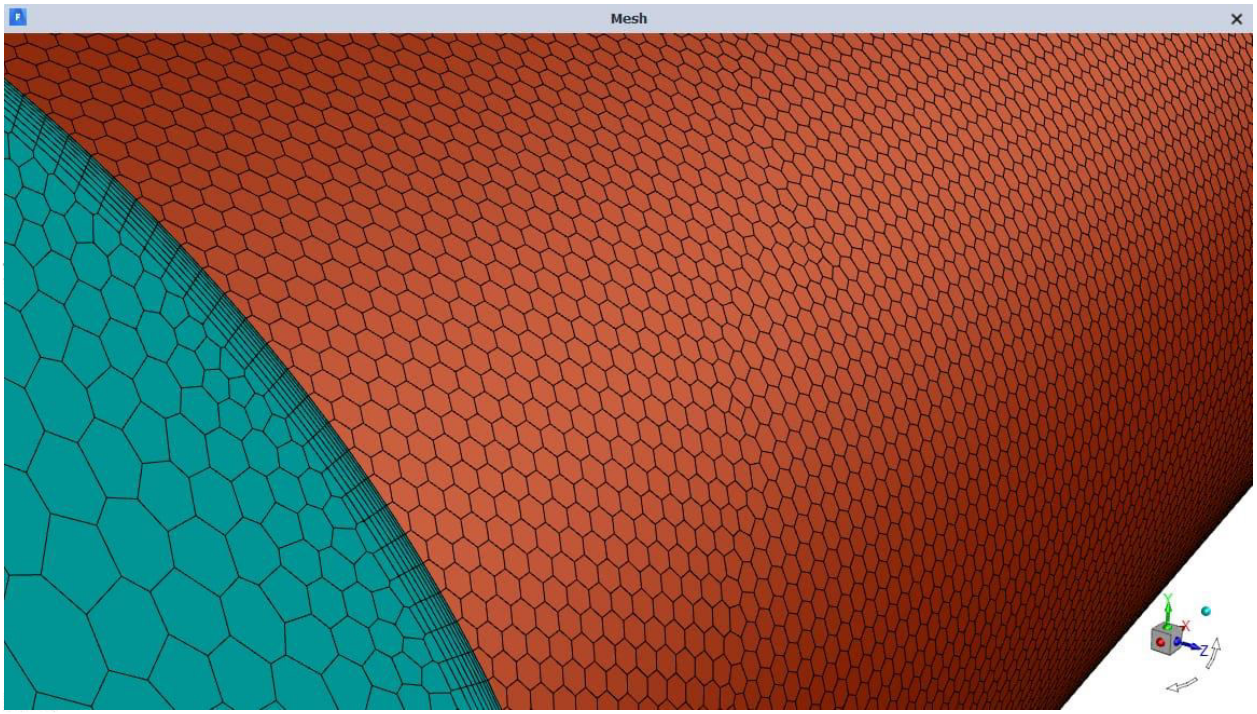

ANALYSIS OF VELOCITY MAGNITUDE AT 200Km/HR

ISSN- 2394-5125 VOL 7, ISSUE 19, 2020

ANALYSIS OF FORCE AT 400Km/HR

Forces - Direction Vector (1 0 0)

	Forces (n)			Coefficients		
Zone	Pressure	Viscous	Total	Pressure	Viscous	Total
wall	-4.4788416	1.8990127	-2.5798289	-0.002369212	0.0010045374	-0.0013646746
Net	-4.4788416	1.8990127	-2.5798289	-0.002369212	0.0010045374	-0.0013646746

ANALYSIS OF FORCE AT 400Km/HR

Forces - Direction Vector (0 1 0)

	Forces (n)			Coefficients		
Zone	Pressure	Viscous	Total	Pressure	Viscous	Total
wall	-9.3685807	0.46577034	-8.9028103	-0.00495578	0.00024638261	-0.0047093974
Net	-9.3685807	0.46577034	-8.9028103	-0.00495578	0.00024638261	-0.0047093974

ANALYSIS OF DENSITY AT 400Km/HR

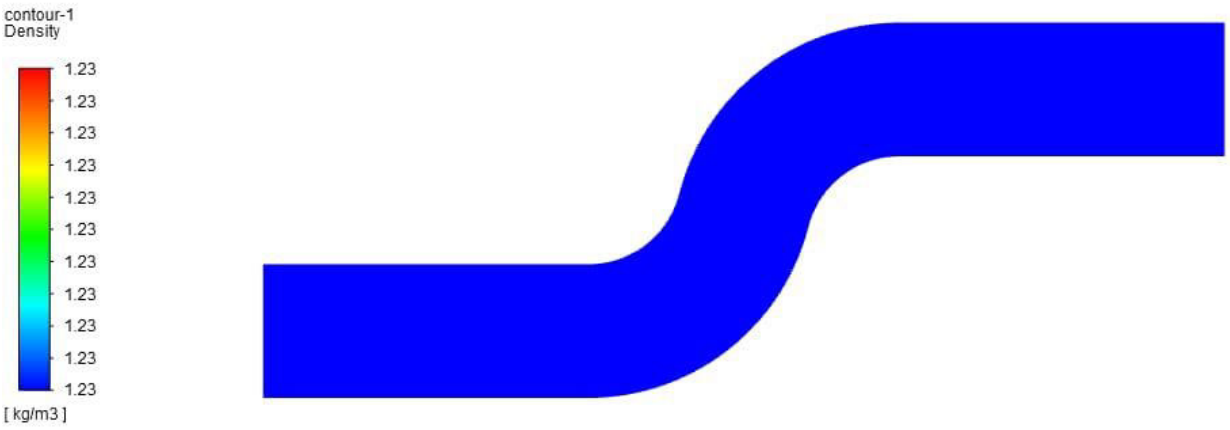

ANALYSIS OF TURBULENT KINETIC ENERGY AT 400Km/HR

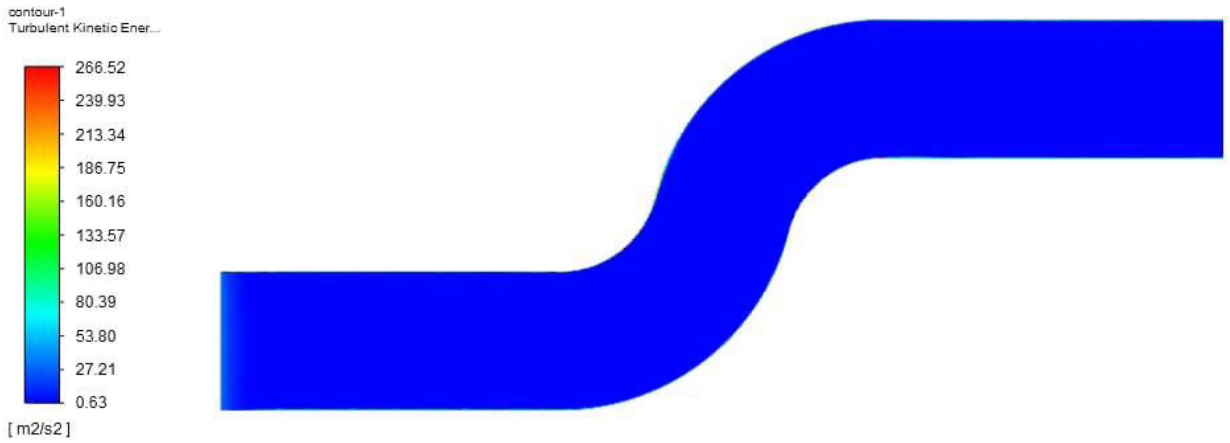

ISSN- 2394-5125 VOL 7, ISSUE 19, 2020

ANALYSIS OF VELOCITY MAGNITUDE AT 400Km/HR

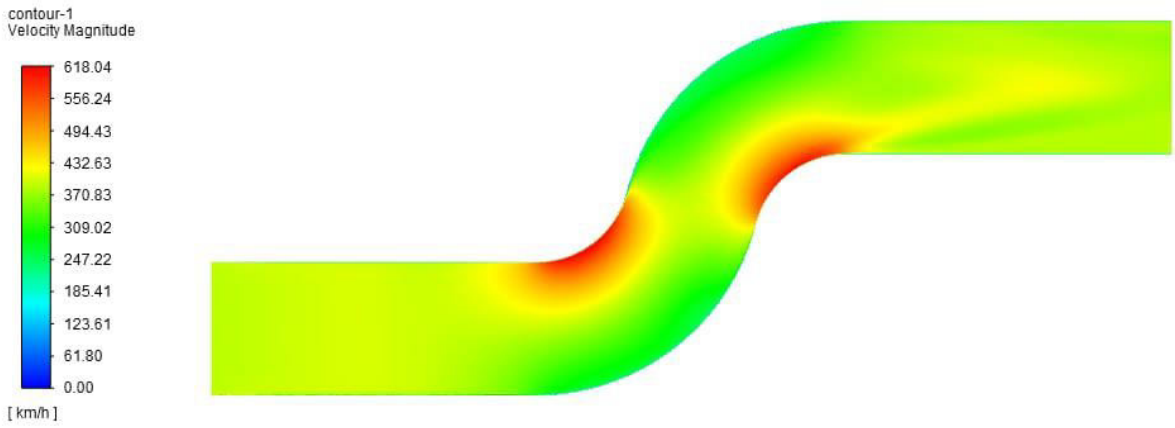

ANALYSIS OF STATIC PRESSURE AT 400Km/HR

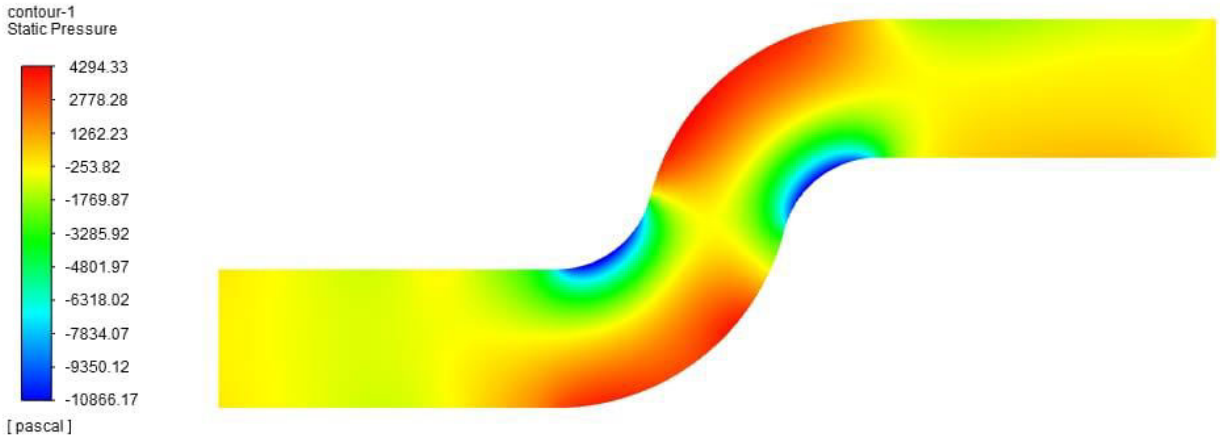

ANALYSIS OF VELOCITY MAGNITUDE AT 400Km/HR

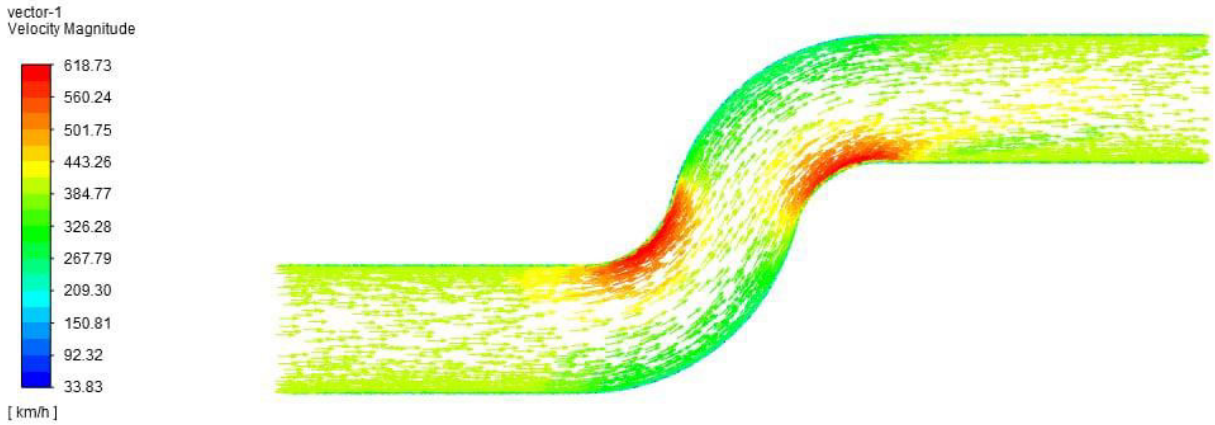

ISSN- 2394-5125 VOL 7, ISSUE 19, 2020

ANALYSIS OF FORCE AT 600Km/HR

Forces - Direction Vector (0 1 0)

Zone	Forces (n) Pressure	Viscous	Total	Coefficients Pressure	Viscous	Total
wall	18.753013	1.0053661	19.758379	0.0099199451	0.00053181732	0.010451762
Net	18.753013	1.0053661	19.758379	0.0099199451	0.00053181732	0.010451762

ANALYSIS OF FORCE AT 600Km/HR

Forces - Direction Vector (1 0 0)

Zone	Forces (n) Pressure	Viscous	Total	Coefficients Pressure	Viscous	Total
wall	8.942499	4.1445432	13.087042	0.0047303919	0.0021923752	0.0069227672
Net	8.942499	4.1445432	13.087042	0.0047303919	0.0021923752	0.0069227672

ANALYSIS OF VELOCITY MAGNITUDE 600Km/HR

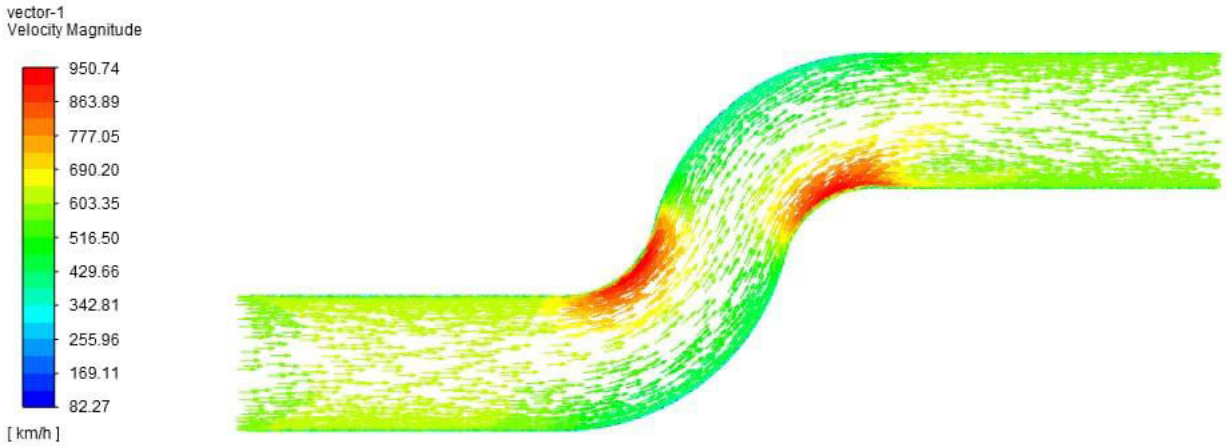

ANALYSIS OF DENSITY AT 600Km/HR

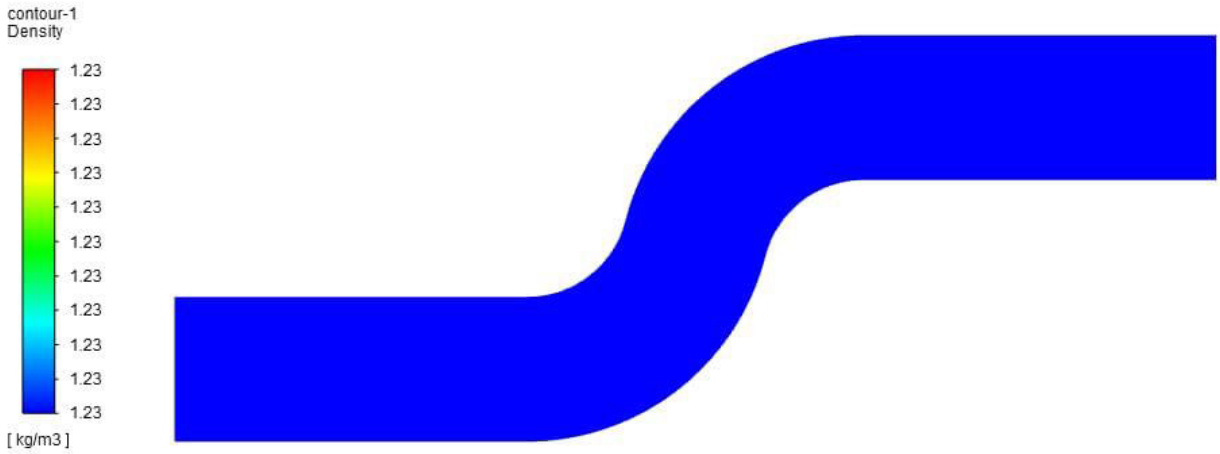

ISSN- 2394-5125 VOL 7, ISSUE 19, 2020

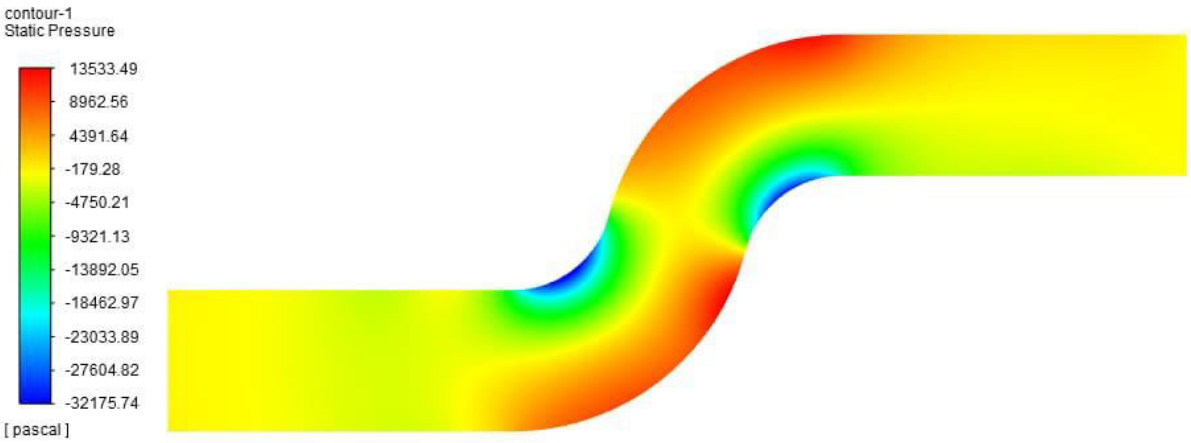

➢ A complicated block-structured topology was used for the grid construction. The blocking topology. The adopted topology enabled the construction of a fine mesh near the engine bullet wall at the engine inlet region.

➢ Appropriate associations were applied between the blocks and the corresponding geometry surfaces or curves in order to keep the surface representation and the mesh density variation as smooth as possible.

➢ The structured grids used in this study contained about approximately 490,000-640,000 polyhedral elements, according to the length of the discretized duct.

➢ The number of elements in each cross-section of the duct was kept almost constant in all cases, with the number of elements in the longitudinal direction varying with the axial length of the duct.

RESULT AND DISCUSSION;

- A parametric CAD model of an S-duct was initially constructed in order to identify the optimal parameters for a duct design for Aircraft and Automobile application.
- Current study Circular section, Rectangular section and Ellipse section S- Duct CAD modelling is drawn as per test with required parameters. The Various speeds (200km, 300km and 400 km) are tested on Ellipse optimized shape.
- The cross sectional areas are same in all shape of S- Duct.
- The CFD analysis conducted on all designs parameters (Static Pressure, Kinetic Energy, Velocity, Density, Drag and Lift)

ISSN- 2394-5125 VOL 7, ISSUE 19, 2020

- Low static Pressure is achived at 300 km speed.
- The density of fluid flow through the S- Duct is same in all kind of speeds (200km, 300km and 400 km)
- The Lower speed (200 km) achieve lower Drag and Low lift values.
- The high speed (400 km) test results shows the drag and lift values are higher than the lower speeds (200km and 300 km).
- The Optimal Ellipse shape is suitable to use low to high speed range in Aircraft and Automobile application.

CONCLUSION;

• A parametric CAD model of an S-duct was initially constructed in order to identify the optimal parameters for a duct design for Aircraft and Automobile application.

• The three different shaped design was adopted in order to decrease the strength of the secondary vortices, which proved to be a good choice.

• Current study Circular section, Rectangular section and Ellipse section S- Duct CAD modelling is drawn as per test required parameters.

• The cross sectional areas are same in all shape of S- Duct.

• The CFD analysis conducted on all designs (Static Pressure, Kinetic Energy, Velocity, Density, Drag and Lift)

1. Anand, R.B., Rai, L. and Singh, S.N. (2003), “Effect of the turning angle on the flow and performance characteristics of long S-shaped circular diffusers”, Proceedings of the Institute of Mechanical Engineering, Part G, Journal of Aerospace Engineering, Vol. 217, pp. 29-41.

2. Baals, D.D., Smith, N.F. and Wright, J.B. (1949), The Development and Application of High-critical-speed Nose Inlets, NACA Report No. 920.

3. Bansod, P. and Bradshaw, P. (1972), “The flow in S-shaped ducts”, Aeronautical Quarterly, Vol. 23, pp. 131-40.

4. Berrier, B.L. and Allan, B.G. (2004), “Experimental and computational evaluation of flush-mounted, S-duct inlets”,

5. 42nd AIAA Aerospace Sciences Meeting & Exhibit Proceedings of the International Conference in Reno, NV, 5-8 January (AIAA 2004-0764).

6. Fluid Dynamics Panel Working Group 13 (1991), Air Intakes for High Speed Vehicles, AGARD-AR-270.

7. Fox, R.W. and Kline, S.J. (1962), “Flow regimes in curved subsonic diffusers”, Transactions of the ASME, Journal of Basic Engineering, Vol. 84, pp. 21-8.

ISSN- 2394-5125 VOL 7, ISSUE 19, 2020

8. Freitas, C.J. (1995), "Perspective: selected benchmarks from commercial CFD codes", Transactions of the ASME, Journal of Fluids Engineering, Vol. 117, pp. 208-18.

9. Goldsmith, E.L., Surber, L.E., Welte, D. and Laruelle, G. (1991), "Chapter 2 – intake design and performance", Air

10. Intakes for High Speed Vehicles, AGARD, AR-270.

11. Grotjans, H. and Menter, F.R. (1998), "Wall function for general application CFD codes", in Papailiou, K.D.,

12. Tsahalis, D., Pe´riaux, J. and Kno¨ rzer, D. (Eds), ECCOMAS 98 Proceedings of the 4th Computational Fluid Dynamics Conference, Vol. 1, Willey, New York, NY, Pt. 2, pp. 1112-17.

13. Guo, R.W. and Seddon, J. (1983), "An investigation of the swirl in an S-duct", Aeronautical Quarterly, Vol. 32, pp. 99-129.

14. Iaccarino, G. (2001), "Predictions of a turbulent separated flow using commercial CFD codes", Transactions of the ASME, Journal of Fluids Engineering, Vol. 123, pp. 819-28.

15. Laruelle, G. and Goldsmith, E.L. (1993), "Chapter 8 – intakes for missiles with air-breathing propulsion", in Goldsmith,

16. E.L. and Seddon, J. (Eds), Practical Intake Aerodynamic Design, AIAA Education Series, American Institute of Aeronautics and Astronautics, Reston, VA.

17. Lee, C.C. and Boedicker, C. (1985), "Subsonic diffuser design and performance for advanced fighter aircraft", AIAA paper, AIAA-85-3073.

18. Majumdar, B., Singh, S.N. and Agrawal, D.P. (1997), "Flow characteristics in S-shaped diffusing duct", International Journal of Turbo and Jet Engines, Vol. 14, pp. 45-57.

19. Menter, F.R. (1994), "Two-equation eddy-viscosity turbulence models for engineering applications", AIAA Journal, Vol. 32 No. 8, pp. 1598-605.

20. Menzies, R.D. (2002), "Investigation of S-shaped intake aerodynamics using computational fluid dynamics", PhD thesis, University of Glasgow, Department of Aerospace Engineering, Glasgow.

21. Mohler, S.R. Jr (2004), "Wind-US flow calculations for the M2129 S-duct using structured and unstructured grids", NASA/CR-2003-212736.

22. Raymer, D.P. (1999), Aircraft Design: A Conceptual Approach, 3rd ed., AIAA Education Series, American Institute of Aeronautics and Astronautics, Reston, VA.

23. Re, R.J. and Abeyounis, W.K. (1996), "A wind tunnel investigation of three NACA 1-series inlets at Mach numbers up to 0.92", NASA TM-110300.

24. Rojas, J., Whitelaw, J.H. and Yianneskis, M. (1983), Developing Flow in S-shaped Diffuser, Part II, Circular Cross-section Diffuser, Department of Mechanical Engineering, Imperial College of Science and Technology, Pub. No. FS/83/28, London.

25. Seddon, J. (1984), "Understanding and countering the swirl in S-ducts. Test on the sensitivity of swirl to fences",

26. Aeronautical Journal, Vol. 32 No. 874, pp. 117-27.

ISSN- 2394-5125 VOL 7, ISSUE 19, 2020

27. Seddon, J. and Goldsmith, E.L. (1999), Intake Aerodynamics, 2 ed., Blackwell Science Ltd, Oxford.

28. Singh, S.N., Seshadri, V., Saha, K., Vempati, K.K. and Bharani, S. (2006), "Effect of inlet swirl on the performance of annular diffusers having the same equivalent cone angle", Proceedings of the Institute of Mechanical Engineering, Part G, Journal of Aerospace Engineering, Vol. 220 No. 2, pp. 129-43.

29. Sonada, T., Arima, T. and Oana, M. (1998), "The influence of downstream passage on the flow within an annular shaped duct", Transactions of the ASME, Journal of Turbomachinery, Vol. 120, pp. 714-22.

30. Taylor, A.M.K.P., Whitelaw, J.H. and Yianneskis, M. (1982), Developing Flow in S-shaped Ducts, I – Square Cross-section Duct, NASA Contractor Report 3550.

31. Tindell, R.H. (1987), "Highly compact inlet diffuser technology", AIAA paper, AIAA-87-1747.

32. Wellborn, S.R., Reichert, B.A. and Okiishi, T.H. (1992), "An experimental investigation of the flow in a diffusing S-duct", NASA Technical Memorandum 105809.

33. Whitelaw, J.H. andYu, S.C.M. (1992), "Flow characteristics in an S-shaped diffusing duct with asymmetric inlet conditions", Proceedings of the 11th Australian Fluid Mechanics Conference, University of Tasmania, Hobart, Australia, pp. 139-42.

34. Yaras, M.I. (1996), "Effects of inlet conditions on the flow in a Fishtail Diffuser with strong Curvature", Transactions of the ASME, Journal of Fluid Engineering, Vol. 118, pp. 772-8.

35. NASA Research Announcement (NRA) Entitled "Research Opportunities in Aeronautics – 2009 (ROA-2009)," NNH09ZEA001N, Release April 13, 2009.

36. Anabtawi, A. J., Blackwelder, R. F., Liebeck, R. H., Lissaman, P. B. S., "An Experimental Study of the Effect of Offset on Thick Boundary Layers Flowing Inside Diffusing Ducts," 30th AIAA Fluid Dynamics Conference, AIAA-99-3590, June, 1999.

37. Brear, M. J., Braddom, S., Warfield, Z., Paduano, J. D., Mangus, J. F., and Philhower, J. S., "Flow Separation Within the Engine Inlet of an Uninhabited Combat Air Vehicle (UCAV)," 4th ASME/JSME Joint Fluids Engineering Conference, No FEDSM2003-45579, Honolulu, Hawaii, July 2003.

38. Florea, R.V., Reba, R., Vanslooten, P. R., Sharma, O., Stucky, M., O'Brien, W. F., Arend, D., "Preliminary Design for Embedded Engine Systems," 47th AIAA Aerospace Sciences Meeting & Exhibit, AIAA-2009-1131, January, 2009.

39. Kirk, A. M., Kumar, A., Gargoloff, J. I., Rediniotis, O.K., and Cizmas, P. G., "Numerical and Experimental Investigations of a Serpentine Inlet Duct", 45th AIAA Aerospace Sciences Meeting & Exhibit, AIAA Paper No 2007-842, January 2007.

40. Hamstra, J. W., Miller, D. N., Truax, P. P., Anderson, B. A., and Wendt, B. J., "Active Inlet Flow Control Technology Demonstration," 22nd International Congress of the Aeronautical Science, No. ICAS-2000-6.11.2, Harrogate United Kingdom, August 2000. Mohler, S. R., "Wind-US Flow Calculations for the M2129 S-Duct Using Structured and Unstructured Grids", 42th AIAA Aerospace Sciences Meeting & Exhibit, AIAA Paper No 2004-0525, January 2004.

ISSN- 2394-5125 VOL 7, ISSUE 19, 2020

41. Mace, J., Lakebrink, M., Mani, M., and Steenken, W., "Computational Simulation of Dynamic Total Pressure Distortion in an S-Diffuser" 48th AIAA/ASME Joint Propulsion Conference & Exhibit, AIAA Paper No. 2012-3999, August 2012.

42. Berrier B. L., and Allen, B. G., "Experimental and Computational Evaluation of a Flush-Mounted, S-Duct Inlet", AIAA Paper No. 2004-0764, January 2004.

43. StarCCM+, Software Package Manual, Ver. 7.02, CD-adapco, Melville, NY, 2011.

44. Menter, F. R., "Two-Equation Eddy-Viscosity Turbulence Models for Engineering Applications," AIAA Journal, Vol. 32, No. 8, pp. 1598-1605, 1994.

45. Allan, B. G., Owens, L. R., and Berrier, B. L., "Numerical Modeling of Active Flow Control in a Boundary Layer Ingesting Offset Inlet", 2nd AIAA Flow Control Conference, AIAA Paper No. 2004-2318, June 2004.

46. Fieldview, Software Package, Ver. 13.1, Intelligent Light, Rutherford, NJ, 2011. Downloaded by PURDUE UNIVERSITY on August 17, 2016 | http://arc.aiaa.org | DOI: 10.2514/6.2013-220 16

47. American Institute of Aeronautics and Astronautics

48. Dubeif, Y. and Delcayre, F., "On Coherent-Vortex Identification in Turbulence," Journal of Turbulence, Vol. 1, No. 11, pp. 1-22, 2000.

49. Nessler, C.A., Copenhaver, W.W and List M., "Serpentine Diffuser Performance with Emphasis on Future Introductions to a Transonic Fan", 51th AIAA Aerospace Sciences Meeting & Exhibit, AIAA Paper, (submitted for publication).

50. Vakili, A., Wu, J.M., Liver, P., and Bhat, M.K., "Measurements of Compressible Secondary Flow in a Circular S-Duct", 16th Fluid and Plasma Dynamics Conference, AIAA Paper No. 83-1739, July, 1983.

51. Wellborn, S.R., Reichert, B.A., Okiishi, T.H., "An Experimental Investigation of the Flow in a Diffusing S-Duct", 28th AIAA/ASME Joint Propulsion Conference & Exhibit, AIAA Paper No. 92-3622, July 1992.

52. Wilcox, D.C., "Turbulence Modeling for CFD", 3rd Edition, DCW Industries, Inc., 2006.

53. Society of Automotive Engineers. "Inlet Total-Pressure-Distortion Considerations for Gas-Turbine Engines," Aerospace Information Report AIR1419, Rev. B, 2007.

54. Society of Automotive Engineers, "A Methodology for Assessing Inlet Swirl Distortion," AIR5686, 2010.

55. Towne, C.E., "Computation of Viscous Flow in Curved Ducts and Comparison with Experimental Data," 22nd AIAA Aerospace Sciences Meeting & Exhibit, AIAA Paper No. 84-0531, 1984. Downloaded